Available online at www.sciencedirect.com

SciVerse ScienceDirect

Procedia Engineering 56 (2013) 702 – 706

Procedia Engineering

www.elsevier.com/locate/procedia

5th BSME International Conference on Thermal Engineering

# Effect of annealing temperature on nanostructured $WO_3$ films on P-Si substrate

M. F. Hossain[a*] and T. Takahashi[b]

[a]Department of Electrical & Electronic Engineering, Rajshahi University of Engineering & Technology, Rajshahi-6204, Bangladesh
[b]Department of Electrical and Electronic Engineering, University of Toyama, Toyama 930-8555, Japan

**Abstract**

Nanostructured WO3 films are prepared on p-Si substrate by facing target sputtering (FTS) method with sputtering pressure, 0.1 Pa and 200W. The sample is annealed at 850°C in air with 5°C/min. The as-deposited and annealed WO3 films have been characterized by the Grazing incidence X-ray diffractometer, Field emission electron microscopy, and Ultraviolet-visible spectrophotometer. The surface morphology of the WO3 films strongly depends on the annealing temperature. An average diameter of the WO3 nanorod is 5-6 µm long and 800 nm diameter. It is revealed from optical study that the band-gap energy of WO3 films is around 2.85 eV. The surface morphology of nanostructured WO3 films has been discussed with the increase of annealing temperature.


Selection and peer review under responsibility of the Bangladesh Society of Mechanical Engineers

*Keywords*: Facing target sputtering,annealed; as-deposited; tungsten oxide; p-Si substrate.

**Nomenclature**

| | |
|---|---|
| $D$ | Crystallite size (nm) |
| $A$ | Edge width parameter |
| *Greek symbols* | |
| $\lambda$ | Wavelength (nm) |
| $\theta$ | Diffraction angle (Deg.) |
| $\beta$ | Full Width Half Maxima (FWHM) |
| $\alpha$ | Absorption coefficient (a. u.) |
| $hv$ | Photon energy (eV) |

## 1. Introduction

Hierarchical self-assembly of nanosized building blocks, including nanowires, nanobelts, nanoplatelets, nanotubes, etc. is an important process for the fabrication of functional electronic and photonic Nanodevices[1]. In this regard, remarkable progress has been made for the synthesis of complex inorganic materials with controlled architectures, sizes, morphologies, and patterns since these parameters represent key elements that determine their electrical and optical properties [2]. Among transition metal oxides, tungsten trioxide ($WO_3$) is of great interest and has been investigated extensively due to its many interesting structural and defect properties. Numerous applications of $WO_3$ optical and electronic based devices include

* Corresponding author.
*Email address:* faruk94_ruet@yahoo.com

1877-7058 © 2013 The Authors. Published by Elsevier Ltd. Open access under CC BY-NC-ND license.
Selection and peer review under responsibility of the Bangladesh Society of Mechanical Engineers
doi:10.1016/j.proeng.2013.03.181

electrochromic (EC) smart windows, flat panel displays, tunable EC photonic crystals [3], gas sensors[4, 5], water splitters, dye sensitized solar cells and batteries. For the fabrication of many of such devices and increasing their efficiencies, nanostructured $WO_3$ films are required to be "thick and porous" enough to provide sufficient volume for producing high interaction areas. Besides, synthesis and assembly of "specific crystallographic phase" can further improve the characteristics of $WO_3$. Tungsten oxide ($WO_3$) is an *n*-type semiconductor and has been investigated extensively owing to their promising physical and chemical properties [6]. $WO_3$ shows good optical properties and proper chemical stability; that is, *Eg* in the range of 2.5–2.8 eV (λ of 400–450 nm) is very suitable for the energy region of visible light [7, 8]. The synthesis of one-dimensional (1D) nanostructures and the assembly of these nano meter-scale building blocks to form ordered superstructures or complex functional architectures offer great opportunities for exploring their novel properties and for the fabrication of nanodevices [9]. Thus for several techniques for the preparation of 1D tungsten oxide nanostructured films have been developed [6].

The deposition of $WO_3$ nanostructured films by facing targets sputtering technique is the newest fabrication method of thin films, with lower particle bombardment compared with the RF sputtering and DC sputtering, because of its special target arrangement. The FTS apparatus are very effective systems for depositing high quality thin films because plasma perfectly confines by the magnetic field between two targets. The thin films can be deposited in non-bombardment by electron ("damage free") conditions [10-12].

In this work, nanostructured $WO_3$ films have been deposited on Si-based substrate by using FTS method with sputtering pressure of 0.1 Pa and annealed at 850°C. The structural, surface morphological properties of nanostructured $WO_3$ films have been investigated and discussed.

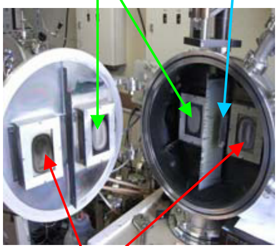


Fig. 1. Facing Target Sputtering system in our laboratory.

## 2. Experimental section

The FTS systems in our laboratory for preparing $WO_3$ thin layer is shown in Fig. 1[13]. The distance between the target-to-target, and the center of the targets' to the substrate were 100 mm and 50 mm, respectively. W rectangular plates (having 115 x 75 mm, thickness of 3 mm and purity of 99.95 %) were used as targets. The chamber was evacuated to a vacuum level of $7\times10^{-4}$ Pa. The $WO_3$ nanoparticles were deposited reactively on Si-based substrate for 2hrs at DC input power of 200 W with sputtering pressure of 0.1 Pa and a fixed Ar to $O_2$ gas ratio ($G_R$) of 6:4 [14]. As-deposited $WO_3$ nanoparticles are annealing in a muffle furnace (TMF5, Thomas) under oxygen environment at 850°C for 2hrs, because as-deposited films are the amorphous structure. The thickness (2 μm) of the $WO_3$ films was determined with a mechanical surface roughness meter (SURFCOM Accretech, 1500 DX) using the step between film and substrate. The crystal structures of the $TiO_2$ films were determined by grazing incident X-ray diffraction (GIXRD) spectra (SHIMADZU XRD-6000) with Cu-Kα line. The data were recorded from 2θ values 20° to 80° with a step of 0.02. For GIXRD measurement incident angle was fixed at 0.45°. The optical properties of the films (prepared on glass substrate) were measured with JASCO V-550 spectrophotometer at room temperature within the wave length range 300-900 nm. The surface morphologies were studied using field emission scanning electron microscope (FE-SEM) with *Model:* JEOL, FE-SEM 6700F.

## 3. Results and discussions

Figure 2 shows the GIXRD patterns of as-deposited and annealed $WO_3$ thin film prepared on Si-based substrate. The GIXRD patterns of the as-deposited $WO_3$ films are found to be amorphous in nature, but crystalline films were obtained when the film is annealed at high temperatures of 850 °C. The lines located at 23.12°, 23.6°, 24.28°, 28.80°, 47.24°, and 50.52° are assigned to the lattice plane reflection of triclinic $WO_3$ phase with lattice parameters $a$ =0.7311 nm, $b$=0.7515 nm, and $c$=0.7679 nm (PC-PDF No. 83-0948). However, triclinic and monoclinic diffraction peaks almost overlap for many 2θ values and it is difficult to discriminate between these two phases. On the other hand, according to the phase diagram, the monoclinic and triclinic structures are the most common and coexist in $WO_3$ at temperatures higher than 500 °C [15]. The crystallite size of the particles has been estimated from the Debye–Scherrer's equation using the GIXRD line broadening as follows [16]: $D = 0.94\lambda/\beta\cos\theta$, where D is the crystallite size, λ is the wavelength of the X-ray radiation (Cu Kα=0.15406 nm), θ is the diffraction angle and β is the FWHM. A finite diffraction peak has been chosen for calculation of crystallite size. The diffraction peak (002) has been chosen for calculation. The derived grain size is 12.3 nm for the annealed $WO_3$ thin films.

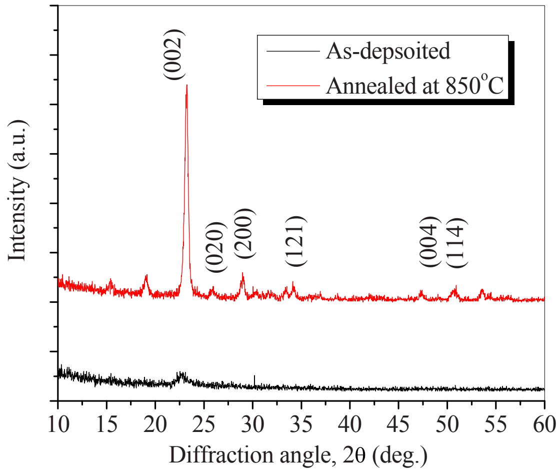


Fig.2. The GIXRD patterns of as-deposited and annealed $WO_3$ thin films

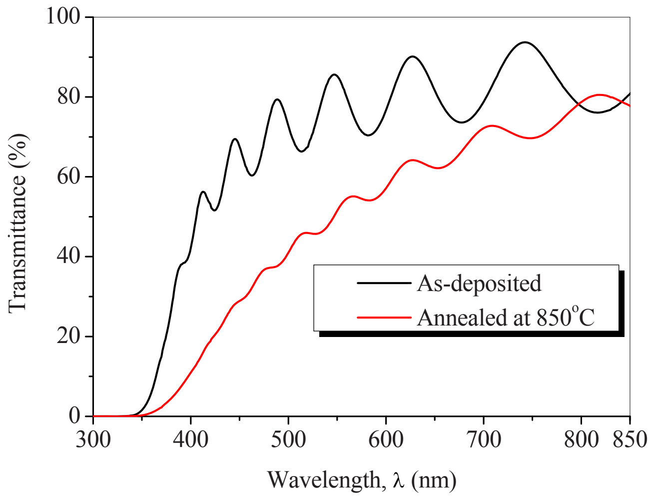


Fig.3. The optical transmittance spectra of as-deposited and annealed $WO_3$ thin films.

Figure 3 shows the transmittance spectra as a function of wavelength (300 - 800 nm) for as-deposited and oxygen-annealed $WO_3$ thin films, prepared in same conditions. The spectra of as-deposited $WO_3$ films show the usual interference pattern in the range of low absorption with a sharp fall of transmittance at the band edge. The oxygen-annealed $WO_3$ thin film is yellowish in color. The oxygen-annealed $WO_3$ films have less interference. It has been observed that the transmittance edge shows the red-shift with the oxygen-annealed $WO_3$ films. It is may be due to the high crystallinity, observed within the sample of investigation. The average transmittance in region varies from 78% to 60.5% with as-deposited and annealed $WO_3$ films, respectively.

We assume an indirect transition between the top of the valence band and the bottom of the conduction band in order to estimate the optical band gap (*Eg*) of the films using the relation [18]: $\alpha(h\nu) \propto A(h\nu - E_g)^2$, where, $\alpha$ is absorption coefficient, $A$ is the edge width parameter and $h\nu$ is the photon energy. Figure 3 shows the plots of $(\alpha h\nu)^{1/2}$ versus the photon energy of the films grown at different sputtering powers. The optical band gap of the films was determined from the extrapolation of the linear plots of $(\alpha h\nu)^{1/2}$ versus hν at $\alpha=0$. The optical band gap of the films is 3.04 and 2.85 eV for as-deposited and annealed $WO_3$ films, respectively.

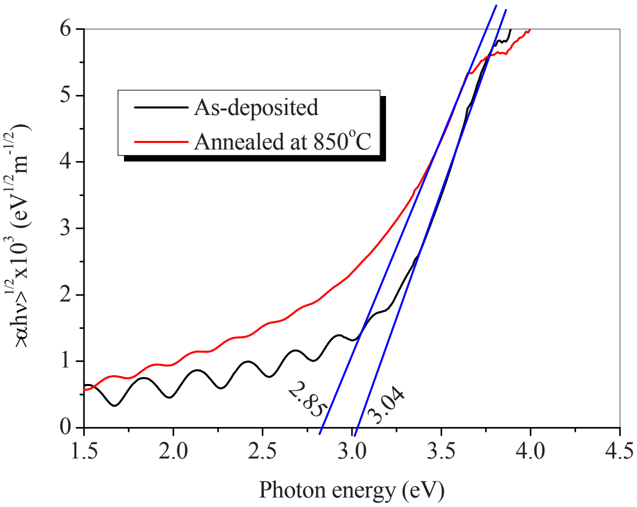


Fig.4. $(\alpha h\nu)^{1/2}$ versus energy for as-deposited and annealed $WO_3$ thin films.

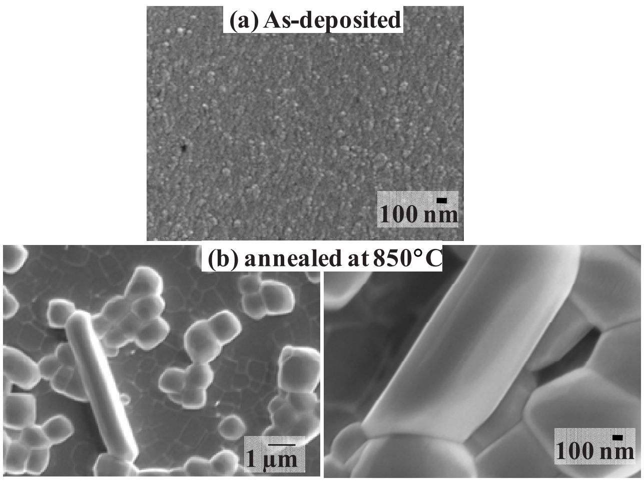


Fig. 5. FE-SEM images of as-deposited and annealed $WO_3$ thin films.

Figure 5 shows the surface structure and morphology of as-deposited and oxygen-annealed $WO_3$ films. From the Fig. 5(a), the as-deposited films have a smooth surface and nanograins are observed in a larger magnification, which reaffirms their amorphous nature. The average-size of the nanograins is 13-17 nm. Oxygen-annealing of the films at 450 °C not only manifests in enhancement of particle size but also in a considerably different surface morphology. It is cleared from the Fig.

5(b) that the whole surface of this film is covered by nanorods and rectangular nanostructures. The average-size of each nanorod is approximately 5-6 μm long and 800 nm diameter. The rectangular shape has cross-section of ~750x~750 nm.

## 4. Conclusion

The nanostructured $WO_3$ films were successfully deposited on Si-based substrate by FTS method with sputtering pressure of 0.1 Pa and annealed at 850°C. High crystalline film is achieved with annealed at high temperature. The whole surface is covered with nanorods and rectangual nanostructures. As-deposited $WO_3$ films have amorphous structure. For the annealed $WO_3$ films, the average-size of each nanorod is approximately 5-6 μm long and 800 nm diameter. The rectangular shape has cross-section of ~750x~750 nm. This nanostructured $WO_3$ films can be used for photocatalytic, electrochromic and solar cells applications. The efficiency of these devices may be enhanced by increasing the thickness of $WO_3$ films.

## Acknowledgement

The authors would like to thank the University of Toyama, for measurement of GIXRD, UV-VIS, FE-SEM and AFM.

## References

[1] Li, S. Z., Zhang, H., Wu, J. B., Ma, X. Y., Yang, D. R., 2006, Crystal Growth Des. 6, p. 351.
[2] Zhang, H., Yang, D. R., Li, D. S., Ma, X. Y., Li, S. Z., Que, D. L., 2005, Crystal Growth Des. 5, p. 547.
[3] Boulmani, R., Bendahan, M., Lambert-Mauriat, C., Gillet, M., Aguir, K., 2007, Correlation between rf-sputtering parameters and $WO_3$ sensor response towards ozone, Sensors and Actuators B, 125, p. 622.
[4] Stankova, M., Vilanova, X., Llobet, E., Calderer, J., Bittencourt, C., Pireaux, J.J., Correig, X., 2005, Influence of the annealing and operating temperatures on the gassensing properties of rf sputtered $WO_3$ thin-film sensors, Sensors and Actuators B, 105, p. 271.
[5] Jimenez, I., Arbiol, J., Dezanneau, G., Cornet, A., Morant, J. R., 2003, Crystalline structure, defects and gas sensor response to $NO_2$ and $H_2S$ of tungsten trioxide nanopowders, Sensors and Actuators B, 93, p. 475.
[6] Li, Y. B., Bando, Y.S., Golberg, D., 2003, Advanced Materials, 15, p. 1294.
[7] Nenadovich, M. T., Rajh, T., Micic, O. I., Nozik, A. J., 1984, Journal of Physics and Chemistry, 88, p. 5827.
[8] Maruska, H. P., Ghosh, A. K.,1978, Solar Energy, 20, p. 445.
[9] Gao, P.X., Wang, Z.L., 2002, Journal of Physics and Chemistry B., 106, p. 126533.
[10] Noda, K.., Kawanabe, T., Naoe. M., 1999, Journal of Magnetics and Magnetic Materrials 193, p. 71.
[11] Nose, M., Nagae, T., Yokota, M., Saji S., 1999, Surface and Coating Technology 116–119, p. 296.
[12] Kim, K.H., Son, I.H., Song K.B., 2001, Applied Surface Science 169–170, p. 410–414, 2001.
[13] Hossain, M.F., Takahashi, T., Ahmed, T., 2011, International Conference on Mechanical Engineering and Renewable Energy, Bangladesh.
[14] Hossain, M.F., Takahashi, T., 2010, Materials Chemistry and Physics 124, p. 940.
[15] Bittencourt, R., Landers, E., Llobet, G., Molas, X., Correig, M. A. P., Silva, J. E., Sueiras, Calderer, J., 2002, Journal Electrochemical Society 149, p. H8.
[16] Cullity, B.D., 1978, Elements of X-ray Diffraction, Addison-Wesley, Reading, MA, USA.